Talanta 116 (2013) 997–1004

Contents lists available at ScienceDirect

Talanta

journal homepage: www.elsevier.com/locate/talanta

Portable integrated microfluidic analytical platform for the monitoring and detection of nitrite

Monika Czugala [a], Cormac Fay [a], Noel E. O'Connor [a], Brian Corcoran [a], Fernando Benito-Lopez [a,b,*], Dermot Diamond [a]

[a] CLARITY: Centre for Sensor Web Technologies, National Centre for Sensor Research, Dublin City University, Dublin, Ireland
[b] CIC microGUNE, Arrasate-Mondragón, Spain

ARTICLE INFO

Article history:
Received 12 June 2013
Received in revised form
15 July 2013
Accepted 24 July 2013
Available online 20 August 2013

Keywords:
Biomimetic microvalve
Low-power analytical platform
Photoswitchable actuators
PEDD detector
Nitrite determination
Microfluidic device

ABSTRACT

A wireless, portable, fully-integrated microfluidic analytical platform has been developed and applied to the monitoring and determination of nitrite anions in water, using the Griess method. The colour intensity of the Griess reagent nitrite complex is detected using a low cost Paired Emitter Detector Diode, while on-chip fluid manipulation is performed using a biomimetic photoresponsive ionogel microvalve, controlled by a white light LED. The microfluidic analytical platform exhibited very low limits of detection (34.0 ± 0.1 μg L^{-1} of NO_2^-). Results obtained with split freshwater samples showed good agreement between the microfluidic chip platform and a conventional UV–vis spectrophotometer ($R^2 = 0.98$, RSD = 1.93% and $R^2 = 0.99$, RSD = 1.57%, respectively). The small size, low weight, and low cost of the proposed microfluidic platform coupled with integrated wireless communications capabilities make it ideal for *in situ* environmental monitoring. The prototype device allows instrument operational parameters to be controlled and analytical data to be downloaded from remote locations. To our knowledge, this is the first demonstration of a fully functional microfluidic platform with integrated photo-based valving and photo-detection.

1. Introduction

Demand for environmental monitoring has grown substantially in recent years in response to increasing concerns over the contamination of natural, industrial, and urban areas with potentially harmful chemical agents. Environmental monitoring by regulatory agencies normally takes place on a manual basis, involving physical sampling and transportation of the samples to centralised facilities equipped with sophisticated instrumentation and analysed by highly trained personnel [1]. Advantages of employing this strategy include high precision and accuracy of the measurements, and adherence to regulatory methods for legal proceedings. However, because of the expense involved in maintaining these facilities and obtaining samples, there are inherent restrictions in terms of the degree of practical spatial and temporal monitoring [2,3]. The use of recent technological breakthroughs may hold the key to addressing these issues. In both research and routine monitoring processes, *in-situ* chemical measurement offers substantial advantages relative to laboratory analysis. Prompt *in-situ* analysis, without human intervention, considerably reduces sample contamination possibilities, improves rates of sample throughput, and facilitates more rapid response to events. Furthermore, the use of autonomous sensor platforms opens opportunities for adaptive sampling of dynamic pollution events, either independently (*e.g.*, through automatic system control of sampling rates) or through human-directed responses (*e.g.*, surface-tethered control of sensor depth), in addition to ensuring substantial reductions in overall cost per measurement.

Characterisation of nutrient distribution within water bodies is critically important because, depending upon their concentrations, they have the potential to greatly disrupt the balance of an aquatic ecosystem. Natural and man-made environmental events can result in dramatic changes in nutrient concentrations in aquatic waters, both in time and geographical distribution. The determination of nitrite (NO_2^-) levels in oceans, rivers, and drinking water is of importance for environmental monitoring agencies since nitrite is both a nutrient and an excretion product of phytoplankton, and it is important with respect to the global nitrogen and carbon cycles, with concomitant effects on climate [4]. The over-use of nitrogenous inorganic fertilisers, combined with the more general mismanagement of natural resources, have caused significant perturbation of both local and global nitrogen cycles [5,6]. The high solubility and mobility of the nitrite and nitrate ions within soil and water have significantly contributed to the eutrophication of lakes and more recently coastal

* Corresponding author. Tel.: +34 943739805; fax: +34 943710237.
E-mail addresses: fernando.lopez@dcu.ie, fbenito@cicmicrogune.es (F. Benito-Lopez).

0039-9140/$ - see front matter © 2013 Elsevier B.V. All rights reserved.
http://dx.doi.org/10.1016/j.talanta.2013.07.058

outfalls. This results in the generation of algal blooms that can wreak havoc with local ecological systems [7]. These problems have been widely recognised, and therefore monitoring the levels of nitrite is of major importance worldwide. Many lab-based analytical methods have been proposed for the determination of nitrite [8,9], but colourimetric methods are by far the most popular [10], due to the excellent limits of detection, dynamic range, and cost efficiency. However, these characteristics can also form the basis of low-cost miniaturised sensors suitable for on-site analysis.

In particular, the spectrophotometric assay based on the Griess reagent has been very popular due to its high stability and sensitivity [11]. Early work in developing platforms for colourimetric sensing based on the Griess reaction was carried out by Greenway et al. [12]. The system utilised electro-osmotic flow (EOF) for pumping and external optical components for absorbance measurements achieving a limit of detection (LOD) of 0.2 mM. Later, Sieben et al. [4] integrated a low cost optical illumination and the detection method with a simple microfluidic system for nitrite detection using the Griess reaction with a limit of detection of 14 nM. Although there are commercial available systems capable of measuring nitrite concentrations, their large physical size (*e.g.* $60 \times 14\ cm^2$) and power consumption (typically greater than 100 W) [13] limit their practical use. Furthermore, due to the reactivity of the nitrite samples, deterioration can rapidly occur, and therefore a strong motivation also exists for the development of on-site measurement systems [4].

An important aspect of environmental analysis is detected by optical methods. Unlike contact based sensors *e.g.* via electrochemical means, optical detection offers several advantages such as the necessity of a reference electrode required for electrochemical sensing, relative insensitivity to electrical interferences and the possibility of remote sensing. As a result, many environmental sensing systems have been reported based on a variety of light sensitive devices such as light dependant resistors [14], photodiodes [15], phototransistors [16,17], and imaging devices (cameras/scanners) [18,19]. However, the energy demands, reliability, and complexity of the sensor can be very significant limiting factors [20]. The paired emitter detector diode (PEDD) device allows overcoming these limitations because it possesses many advantages such as low cost, high resolution, increased sensitivity, ease of implementation, and a relatively low power demand. Recently it was shown that light emitting diodes (LEDs) based systems can be used for applications where high sensitivity is an absolute requirement [21].

In recent years, advances in microfluidic techniques for environmental applications have opened opportunities for improvements in water quality monitoring [4]. However, the development of fully integrated microfluidic devices capable of performing complex functions requires the integration of microvalves with an appropriate performance, as they are essential tools for the control and manipulation of flows in microchannels [22]. The issue of liquid handling is a key factor inhibiting chemo-/biosensor network deployments for applications involving liquid-phase measurements such as water quality monitoring, due to the cost and power demand of conventional valves, and their necessary use in off-chip configurations. Stimuli responsive materials, actuated by light irradiation, can significantly facilitate liquid movement within microfluidic devices. Several research groups have reported flow valves based on thermoresponsive poly(*N*-isopropylacrylamide) (pNIPAAm) polymer gels [23,24]. The fluid containing the block copolymer of poly(*N*-isopropylacrylamide-co-n-butyl methacrylate) and poly (ethylene glycol) was introduced into the microchannel, and the direction of the fluid was controlled by local sol–gel transformation of the polymer induced by infrared laser irradiation as strong as 650 mW. Fluid manipulation by ultraviolet (UV) [25] or 785 nm laser light [26] irradiation induced surface wettability change was also presented. Although the method is simple to manipulate fluids on microchips, once the channel is wetted with the fluid, it is difficult to stop the fluid. Sershern et al. [27] demonstrated light controlled nanocomposite hydrogel microvalves composed of pNIPAAm gels containing nanoparticles that have strong optical absorption. Optical energy from a laser light irradiation as strong as 1600–2700 mW cm^{-2} was transformed into heat by the nanoparticles, which induced shrinkage of the thermoresponsive pNIPAAm gels and the opening of microvalves. Although the fluid manipulation by light irradiation was successfully achieved, heat transfer between microvalves may well be a problem for controlling multiple integrated microvalves. Moreover, application of heat induced volume transition may not be suitable for the manipulation of fluids containing heat sensitive materials, such as proteins or cells. On the other hand, stimuli responsive microvalves based on pNIPAAM gels functionalised by spirobenzopyran chromophores (pSPNIPAAm) present an interesting option for fluid manipulation. Several groups have reported pSPNIPAAm gel microvalves, fabricated by *in-situ* photopolymerisation in the microchannel, and independently controlled by local light irradiation [28,29]. These photo-controlled microvalves provide non-contact, spatially independent and parallel fluid manipulation. Using ionogels rather than hydrogels, the physical robustness of the photoswitchable materials is increased. In contrast to conventional p(SPNIPAAm) hydrogels, which tend to physically collapse when dry, ionogels are protected from drying and cracking because of the negligible vapour pressure of the ionic liquid (IL) at room temperature. These polymer actuators can be integrated into microfluidic devices, providing a route to 'biomimetic' microfluidic systems that are inherently low power, and potentially more reliable in microchannels than equivalent conventional micro-engineered actuators [2].

In this paper, we report, for the first time, the design, fabrication and testing of a wireless, portable, integrated microfluidic analytical platform for point-of-care monitoring and quantitative determination of nitrite in freshwater samples. The miniaturised gold-standard Griess assay is implemented for detecting nitrite within a poly-(methylmethacrylate) (PMMA) microfluidic device. The platform integrates optical fluid processing and detection, enabling monitoring of the kinetics of the Griess reaction and the detection of nutrient levels. For fluid control, the microfluidic device contains a biomimetic photo-switchable microvalve based on a phosphonium ionogel functionalised with spiropyran. The microvalve is simply actuated by illumination with a light emitting diode. In addition, the nitrite concentration is determined by a highly sensitive, low cost wireless PEDD detector, ensuring inexpensive fabrication and functioning of the whole platform.

2. Experimental

2.1. Chemicals and reagents

All solutions were prepared from analytical grade chemicals and deionised water from a Millipore Milli-Q Q-GARD® 1 water purification system. Stock solutions were prepared freshly prior to use and stored in dark environment at room temperature for no longer than one week. The Griess reagent was prepared following this procedure: Firstly, a 5% phosphoric acid solution was prepared by dissolving 5 g of phosphoric acid (H_3PO_4) in 100 mL of deionised water. Next, a 1% sulfanilic acid solution was prepared by dissolving 1 g of sulfanilic acid in 100 mL of a 5% phosphoric acid solution. A 0.1% *N*-(1-naphthyl)ethylenediamine dihydrochloride (NED) solution was prepared by dissolving 100 mg of NED in 100 mL of deionised water. Finally, 1% sulfanilic acid solution and 0.1% NED solution were mixed together forming a Griess reagent. A sodium nitrite ($NaNO_2$) stock solution was prepared by dissolving 0.3 g of $NaNO_2$ in 500 mL of deionised water. Nitrite standard solutions were diluted from a 200 mg L^{-1} $NaNO_2$ stock solution to the appropriate concentrations. Phosphoric acid, sulfanilic acid, *N*-(1-naphthyl)

ethylenediamine dihydrochloride and sodium nitrite were purchased from Sigma-Aldrich®, Ireland and used without further purification.

For ionogel microvalve preparation *N*-isopropylacrylamide, *N*,*N*'-methylene-bis(acrylamide) (MBAAm), 2,2-5 dimethoxy-2-phenyl acetophenone (DMPA) were used and purchased from Sigma-Aldrich®, Ireland. 1′, 3′, 3′-Trimethyl-6-hydroxyspiro(2H-1-benzopyran- 2, 2′-indoline) (Acros Organics, Geel, Belgium), 3-(Trimethoxysilyl) propyl methacrylate was purchased from Sigma-Aldrich®, Ireland. Trihexyltetradecyl-phosphonium dicyanoamide [$P_{6,6,6,14}$][dca] was obtained as compliments of Cytec® Industries, Ontario, Canada. Further purification was carried out as follows: 10 mL of IL decolourised by redissolution in 30 mL of acetone followed by treatment with activated charcoal (Darco-G60, Aldrich) at 40 °C overnight. Carbon was removed by filtration through alumina (acidic, Brockmann I, Aldrich) and the solvent removed under vacuum at 60 °C for 24 h at 0.1 Torr. A liquid prepolymer mixture was prepared by dissolving the NIPAAm monomer (0.75 mmol), the MBAAm (0.04 mmol), acrylated spirobenzopyran monomer (0.01 mmol) and the photo-initiator DMPA (0.02 mmol) into the ionic liquid (0.52 mmol).

2.2. Microfluidic device fabrication

The microfluidic device consists of a multi-layer structure made of poly(methyl methacrylate) and pressure-sensitive adhesive (PSA) sheets. Using a laser ablation system-excimer/CO_2 laser (Optec Laser Micromachining Systems, Belgium) reservoirs and microchannels were machined into the PMMA (Radionics, Ireland) along with 50 μm and 86 μm thick double-sided, pressure-sensitive adhesive layers (PSA, Adhesives Research, Ireland). Once the appropriate pieces had been designed and machined, they were aligned and bonded using a thermal roller laminator (Titan-110, GBC Films, USA).

The ionogel microvalves were photopolymerised *in-situ* in a circular reservoir (500 μm radius; V_{IL}=177 nL) for 25 min using a UV irradiation source (λ=365 nm) placed 8 cm from the solution (UV intensity 10 mW cm^{-2}). When polymerisation was complete, the resulting ionogels were rinsed with deionised water to remove any un-polymerised monomer and excess of ionic liquid. The photopatterned ionogel microvalves were dried at room temperature for 24 h. Finally, the top PMMA layer was bonded to the microfluidic. Fig. 1A shows the microfluidic device fabrication procedure. After assembly the upper part of the microchannel (Y – branches) was then filled with 1 mM HCl aqueous solution and kept for 2 h at 21 °C for swelling of the pSPNIPAAm ionogels (closing of the microvalve).

The microfluidic device consisted of a small structure of 20×30 mm^2 dimension, as shown in Fig. 1B. Round inlets for water sample (radius 2.25 mm) and for Griess reagent (radius 250 μm) are placed at the top of the Y-shaped channel. The junction of the collecting channels with the integrated microfluidic microvalve was followed by the mixing part of the channel which had a total length of 72 mm length and 1 mm wide. The detection chamber (radius 2.4 mm) was followed by a 1 mm width channel to the outlet/waste area, which was connected with the back pressure system.

2.3. Portable, integrated microfluidic analytical platform fabrication

The control, communications, and detection system were designed to be compatible with the fabricated microfluidic device. A cradle was designed using 3D CAD software (Pro Engineer 4.0) to hold and restrain the microfluidic device during envisaged operational conditions. Fig. 2 presents the cradle consisting of three brackets to align the LEDs, with the locations of the microvalve and the detection area, see Fig. 1. The cradle parts were manufactured using a rapid prototyping system (Dimension SST 768) using a black polymer formulation to reduce interference due to external light fluctuations or internal reflections.

Fig. 3 shows the control and communication sub-systems responsible for operation of the device. A microcontroller board (with an MSP430 F449, Texas Instruments, at its core) was designed, created, and programmed in order to accept user commands (*e.g.*, turn on/off the LEDs), and to quantify the transmitted light through the reagent/sample mix (Fig. 3A). A 3.7 V lithium-ion battery (Panasonic PAL2) with a low form factor provided power to the portable unit and was regulated to a constant 3.3 V via an on-board, low noise, voltage regulator (LP2985, Texas Instruments), sourced from Farnell, Ireland. The 3.3 V source also supplied power to the white and green LEDs, which was important for maintaining constant illumination conditions [30].

Communications between the operator and the microcontroller was achieved through two wireless radio transceivers (EZ-Radio ER900TRS, LPRS) with one located at the base station (connected to a PC/Laptop through a FDTI UB232R USB interface, Fig. 3B) and the other connected to the microcontroller *via* UART protocol [31]. Users/operators executed pre-programmed subroutines on the microcontroller *via* a command line interface, which was enabled through a terminal programme on a PC/Laptop; Hyperterminal was used for this purpose. In addition, data harvested by the detector was wirelessly streamed to the PC/Laptop in real time where it was continuously saved to file for future analysis. Each data point was time stamped *via* a real time clock (32 KHz crystal, C-001 R, Epson Toyocom).

Colourimetric detection was achieved through the use of the aforementioned LEDs, *i.e.* green (emitter, 540 nm, Radionics,

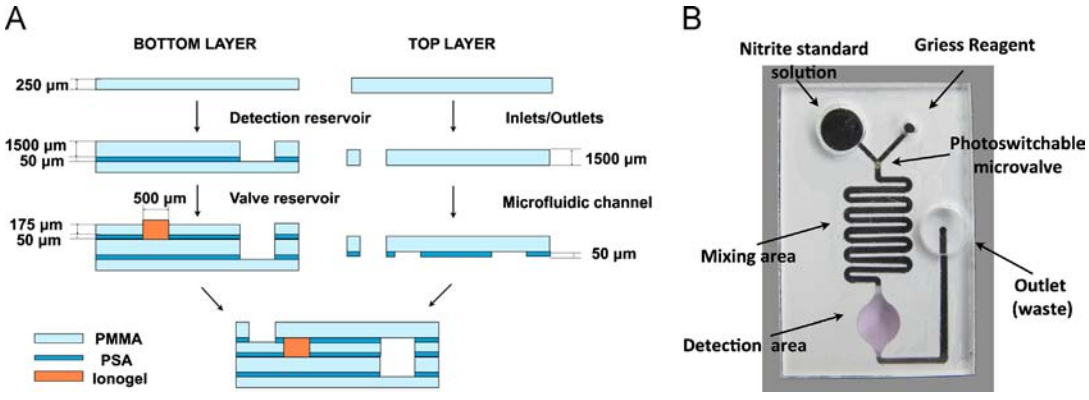

Fig. 1. (A) Schematic representation of the microfluidic device fabrication procedure. (B) Picture of the microfluidic device fabricated in PMMA: PSA polymer by CO_2 laser ablation.

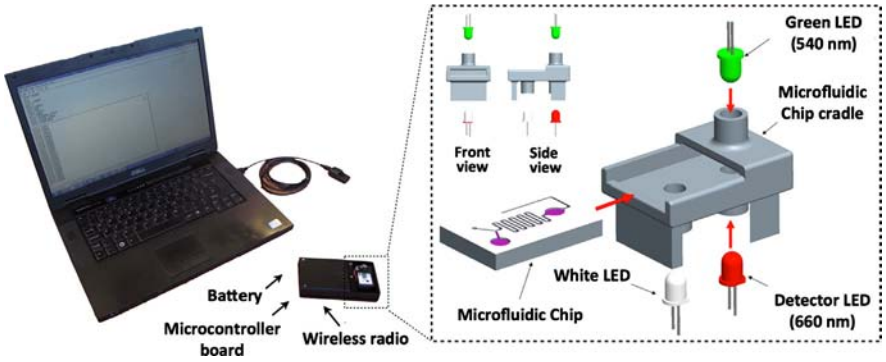

Fig. 2. Computer with the wireless, portable, integrated microfluidic analytical platform (left) and CAD assembly model showing the microfluidic cradle (right), microfluidic device along with the white LED (actuate valve) and the PEDD detector LEDs (green-emitter and red-detector) positioning. Side and front views are also provided (right side, top left). (For interpretation of the references to colour in this figure legend, the reader is referred to the web version of this article.)

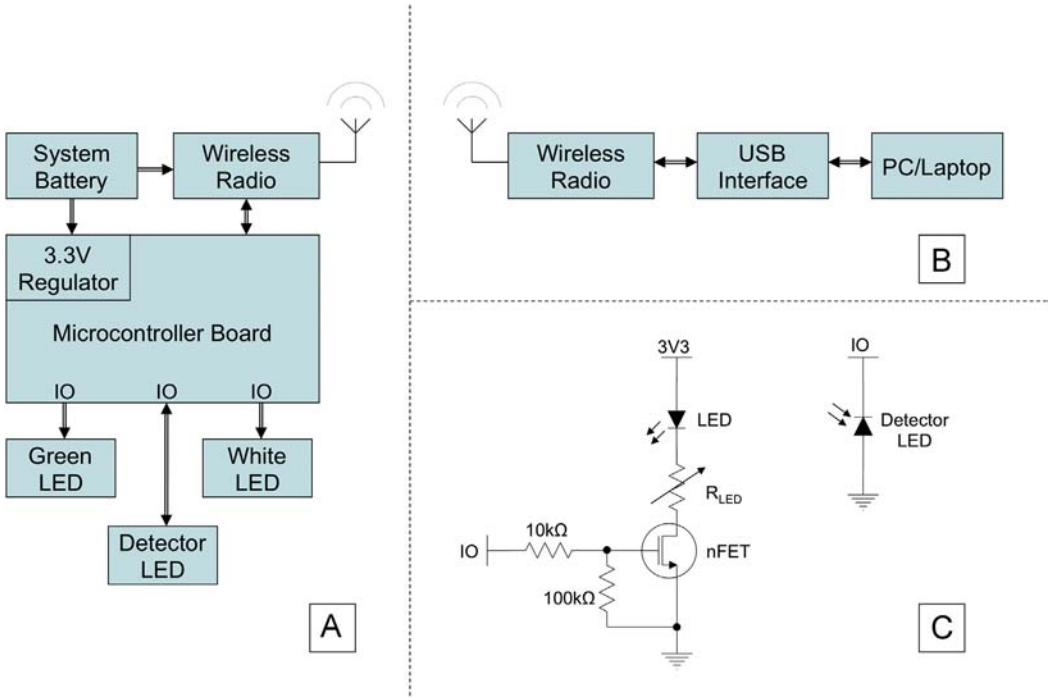

Fig. 3. Device design. (A) Block diagram representation of the wireless analyser (B) Block diagram of the base station. (C) Schematic of the circuitry to actuate the power to the emitter LEDs (left) and connexion of the detector LED (right).

Ireland) and red (detector, 660 nm, Radionics, Ireland), arranged in absorbance/transmission mode as shown in Fig. 2. Light generated by the emitter was partly absorbed by the Griess-nitrite complex, which absorbs strongly around 540 nm (λ_{max}=547 nm) [32]. Hence the photon flux reaching the reverse biased detector LED depends upon the concentration of nitrite within the sample. This in turn generates a photo current from the reverse biased detector diode [33], which discharges a pre-set capacitance. The time taken to discharge the capacitance depends on the photocurrent generated by the detector LED, which in turn depends on the nitrite concentration in the sample, as described by Lau et al. [34] Accurate determination of the discharge time is achieved via a software counter within the microcontroller that accumulates the number of times the signal is above the I/O port's logic 0 (discharged) threshold over a fixed duration [30]. A time delay was implemented between each increment of the counter. This was determined experimentally by introducing the desired maximum and minimum concentrations into the microfluidic device in order to optimise the resolution for a 16-bit software counter *i.e.* in the range of 0–65535.

2.4. Measurement protocol

For conditioning the microvalve, 1 mM HCl solution was introduced to the microfluidic channel allowing the ionogel to swell for 2 h in a dark environment. After microvalve actuation (contraction) triggered using the white light LED (Radionics, Ireland), nitrite detection was achieved via the Griess method [35]. The sample to reagent ratio adopted throughout all the experiments was 15: 1 v/v [32]. Measurements were obtained by introducing 34.5 μL nitrite standard/sample/water and 2.3 μL Griess reagent into their respective storage reservoirs on the microfluidic device, inlets (Fig. 1B). Using 25 mbar back pressure from a vacuum pipe connected to the microfluidic device *via* the outlet, the liquids were moved from the storage reservoirs and allowed to mix through the serpentine reaction microchannel as they moved towards the detection chamber (flow rate=0.03 μL min^{-1}), wherein the concentration measurement took place. After the detection chamber was filled, see Fig. 1B, the intensity of the coloured solution was determined using the PEDD detector. The detector sampling rate under this protocol was set at 1 Hz.

For comparison, the calibration curve using UV–vis spectrometer was carried out using the same nitrite standards/samples/water and Griess reagent mixtures pipetted into the cuvette. The development of the nitrite Griess reagent complex colour intensity was monitored, range 0.0–1.2 mg L^{-1} NO_2^-, using a Perkin-Elmer Lambda 900 spectrophotometer by taking an absorbance measurement at 540 nm for 40 min (T=21 °C). Each experiment was carried out in triplicate.

3. Results and discussion

3.1. Volume phase transition of the photo-switchable ionogel microvalve

Fig. 4 shows the volume phase transition of a pSPNIPAAm ionogel disc induced by white light irradiation. From an initial height of 250 μm after photo-polymerisation, the ionogels reached a height of 395 μm after swelling for 2 h in HCl (1 mM) solution, exhibiting an increase of ~58% from its initial dimensions. Before white light irradiation, the swollen pSPNIPAAm ionogel had a strong yellow colour due to the protonated open-ring form of the spirobenzopyran chromophore (MC-H^+), Fig. S1. Upon irradiation with white light, isomerisation to the closed-ring form (SP) was induced, and the yellow colour faded, followed by dehydration contraction of the pSPNIPAAm ionogel. It was found that the height of the ionogel microvalve typically contracts by about 42% of its initial swollen state after white light irradiation (30 min) in 1 mM HCl (pH=3) at 21 °C.

In order to achieve effective fluid movement control, the photo-induced contraction of the ionogel must create an open channel (contracted gel) from a previously closed channel (swollen ionogel). To investigate this, 1 mM radius circular reservoirs with depths ranging from 200 to 300 μm were fabricated in the bottom layer of the microfluidic device (Fig. 1A), and then filled with the ionogel solution. The microvalves were photopolymerised with UV light, as described above, and their actuation in the microfluidic device investigated. It was found that microvalves prepared using 200 μm deep reservoirs were too small to block the channel after swelling, while microvalves prepared using 300 μm deep reservoirs were too large in their swollen state, and the microvalves did not open even after prolonged exposure (2 min) to white light irradiation. It was found that 1 mm radius valves formed in 225 μm reservoirs (Fig. 1) gave a nice balance between effective blockage of the channel in the swollen state, and reasonably rapid opening of the channel when the valve was illuminated using the white light LED (see below).

3.2. Fluidic control in the microfluidic device

Fig. 2 shows the basis arrangement for operation of the photo-responsive gel microvalve. Initially, the microvalve is in the closed (swollen) state, thus blocking the channel (Fig. 5, left). When the pSPNIPAAm ionogel is irradiated with white light from the LED (intensity 1 W cm^{-2}), photo-induced shrinkage occurs, and the microvalve opens after 30 ± 5 s (n=3, Fig. 5, right). The microvalve was found to be unaffected by pressure up to 31 ± 4 mbar (n=3) at which point they deformed and failed.

After opening of the microvalve, the water sample and Griess reagent move from the reservoirs towards the serpentine mixing region. Preliminary experiments showed this design ensures efficient mixing of the sample and reagents. Fig. S2 demonstrates the effectiveness of the mixing process, which is essentially complete after *ca.* 10 mm (after the second channel loop). The sample then continues through the microfluidic device to the detector region where the absorbance of the LED radiation is measured at *ca.* 540 nm.

Fig. 4. Photo-switchable ionogel after photopolymerisation (A), swelling in 1 mM HCl for 2 h (B) and shrinking upon white light irradiation (C).

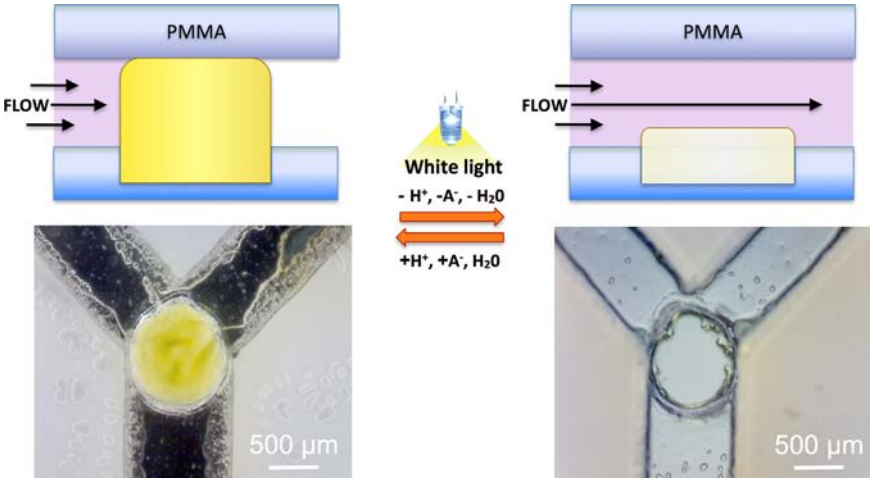

Fig. 5. Schematic (top) and images (bottom) of the photoresponsive microvalve in closed (left) and opened (right) state.

3.3. Portable, integrated microfluidic analytical platform characteristics

The microfluidic device presented in this study was integrated into a portable analytical platform that incorporated all the features necessary to actuate the microvalve, perform reagent/sample mixing, measure the colourimetric response, and transmit the harvested data wirelessly to a remote base station.

3.3.1. Reagent consumption

Typical flow injection analysis (FIA) systems employing the Griess method for nitrite detection consume relatively large amounts of reagent (approx. 5–20 mL per sample) [4] making the technique rather difficult to scale up. In contrast, the prototype platform only requires *ca.* 2.3 μL of Griess reagent per assay, resulting in significant reduction in costs associated with reagent purchase, servicing visits, platform size, power consumption and waste disposal.

3.3.2. Microvalve actuation

The photo-switchable ionogel microvalve is very low cost to produce in terms of materials, and its fabrication via *in situ* photopolymerisation opens the possibility of creating complex microfluidic structures incorporating large numbers of valves. Furthermore, as it is actuated using light, no physical contact is required with the actuating stimulus, and therefore the microfluidic system can be completely sealed from the electronics, and the valve structures subsequently introduced. The white light intensity used to control the pSPNIPAAm ionogel microvalve in the current arrangement is *ca.* 1 mW cm^{-2}, which is substantially smaller than previously reported optically controlled nanocomposite hydrogel microvalves (> 1600 mW cm^{-2}) [36]. For comparison, the power consumption of typical miniature conventional solenoid valves (TX3P006, Sensor Technics; 600 mbar) is up to 500 mW. Moreover, the white LED used is a standard off-the-shelf component costing *ca.* €0.80 keeping the actuation at a low cost.

The reusability of the whole platform depends strongly on the performance of the ionogel microvalve. In its current configuration the ionogel microvalve was actuated up to three times without showing any sign of feature.

3.3.3. Detection system

As previously stated, the detection system was based on a paired emitter detector diode set-up. The emitter 540 nm LED wavelength was chosen to be compatible with the Griess reagent-nitrite azo dye absorption spectrum (λ_{max}=547 nm), whereas the 660 nm LED was used as a detector because it was previously demonstrated that in the PEDD configuration, the reverse biased detector LED is sensitive to light of wavelength equal to or greater than the emission wavelength [34]. As the PEDD circuit generates a digital output from the counter (16-bits in this case, but can utilise 32-bits if required), which is greater resolution than a standard 10 or 12 bit ADC channel. In addition, the detector basically integrates the signal over a fixed time interval, noise is inherently supressed, and extremely low detection limits can be obtained [32]. Finally, the platform can be easily reconfigured for colourimetric detection at other spectral regions by changing the emitter LED.

Another significant advantage of this detection system is its low-cost feature. As LEDs are inexpensive and can be obtained off-the-shelf in a broad range of sizes and wavelengths [37], this is an attractive detector strategy that can be implemented for a broad range of analytes [34]. In the context of colourimetric chemical detection a common implementation is based on photodiodes, for comparison. Photodiodes are by far one of the most commonly used detectors in optical sensing [38]. However, its implementation is higher in cost and complexity as it requires Op Amps with additional components, an available analogue to digital converter (ADC) on the microcontroller and a higher power requirement. A comparison of both approaches has already appeared in a study by O'Toole et al. [39], who emphasised the advantage of the PEDD implementation.

3.3.4. Communications

Many microcontroller devices using wireless modules are electing for the 2.4 GHz ISM band [40]. There are good reasons for this, one of which is the cost effective nature of device construction as this band has become increasing popular due to pervasive technologies such as Zigbee, WiFi, 3G, *etc.* However, it was decided to modularise this platform at the design stage to allow for ease of integration into other available networks, if required at future stages. However, for environmental applications the 900 MHz radio band offers the advantage over the 2.4 GHz band as it is capable of communicating around objects such as trees, or the landscape, *etc.*, all of which can be attenuated at 2.4 GHz [41].

3.4. Portable, integrated microfluidic analytical platform performance

To demonstrate the utility of the portable integrated microfluidic analytical platform, the system was applied for the determination of nitrite levels in water samples. In colourimetric reagent based reactions, the reaction kinetics defines the time allowed for the sample to react with the reagent in the manifold. The kinetic curves obtained from the prototype platform are presented in Fig. S3. The signal (discharge time) *versus* time curves for the NO_2^- concentrations were modelled using a first order exponential equation (Eq. 1):

$$D_t = a \times (1 - e^{(-kt)}) \quad (1)$$

where D_t is the discharge time (μs) at the end of the reaction, a is a scaling factor, k is the first order rate constant (s^{-1}) and t=time (s).

First-order kinetic models were fitted (Microsoft Excel Solver) [42] to each of the curves and the rate constants were calculated over the concentration range 0.0–1.2 mg L^{-1} of NO_2^-. The average response (n=3) and fitted models are presented in Fig. 6A. It was found that for nitrite concentrations higher than 0.4 mg L^{-1} and at a flow rate of flow rate of 0.03 μL min^{-1}, the reaction had already commenced by the time the data acquisition was initiated. This is due to the efficient mixing provided in the serpentine microchannel region, which caused the nitrite Griess reagent complex to rapidly form in the serpentine channel region at higher concentrations. This effect can be reduced by increasing the flow rate. When the reaction mixture reaches the detection chamber, signal acquisition is initiated. In Fig. 6 it can be seen that the colour formation increased rapidly at all concentrations until approximately 20 min after which a steady state signal was observed. Therefore this reaction time was adopted for all further experiments.

Calibration plots obtained with the prototype platform were found to be linear up to 1.2 mg L^{-1} of nitrite (R^2=0.98, RSD=1.93%, n=3). The responses were plotted against the nitrite Griess reagent complex concentration using Eq. 1 and the results are presented in Fig. 6B. The LOD, calculated as the concentration of nitrite which produced an analytical signal three times the standard deviation of the blank, was estimated as 34.0 ± 0.1 μg L^{-1} nitrite, and the limit of quantification (LOQ), calculated as the concentration of nitrite which produced an analytical signal ten times the standard deviation of the blank, was 115.2 ± 3.1 μg L^{-1}.

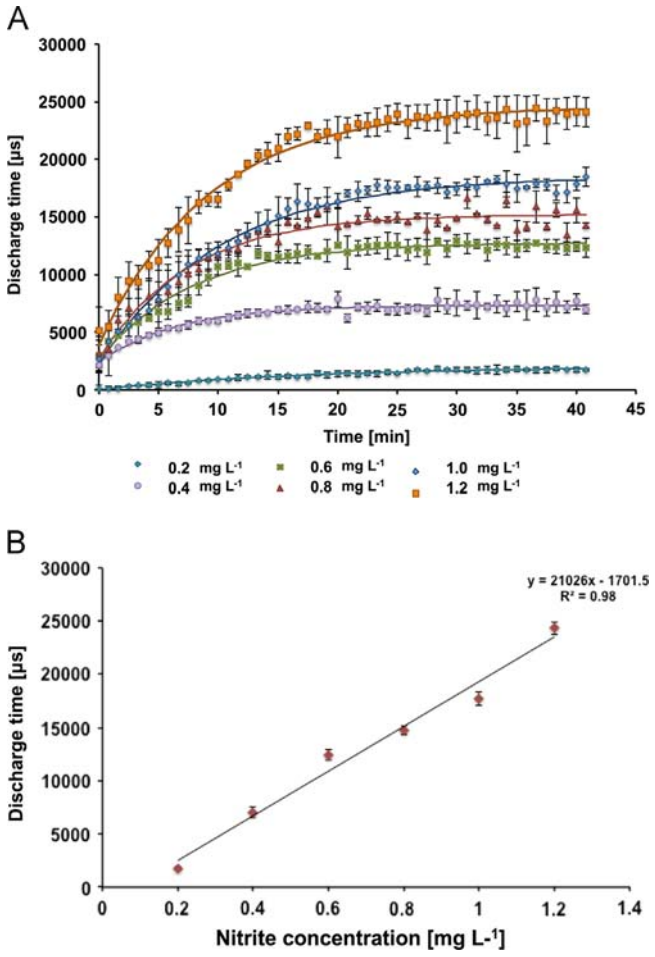

Fig. 6. (A) Kinetic study of colour formation using a 540 nm emitter LED for the nitrite Griess reagent complex formation ($n=3$) and (B) calibration plot from the same data taken at $t=40$ min.

Table 1
Comparison of the data obtained for the detection of nitrite Griess reagent complex using both the portable, integrated microfluidic analytical platform and a UV–vis spectrophotometer ($n=3$).

	Microfluidic analytical platform (540 nm)	**UV–vis spectrophotometer** (540 nm)
R^2	0.98	0.99
LOD	34.0 ± 0.1 µg L^{-1}	1.50 ± 0.02 µg L^{-1}
LOQ	115 ± 3 µg L^{-1}	14.8 ± 0.2 µg L^{-1}
RSD	1.93%	1.57%

For comparison, the absorbance of the same Griess reagent/nitrite solutions was measured using a UV–vis spectrophotometer. As shown in Fig. S4, the absorbance at 540 nm plotted against nitrite Griess reagent complex concentration gave a linear range ($R^2=0.99$) of 0.0–1.2 mg L^{-1} with an RSD=1.57%, $n=3$, LOD=1.50 ± 0.02 µg L^{-1} and LOQ=14.8 ± 0.23 µg L^{-1} (Table 1). The difference in LOD/sensitivity is primarily due to the much smaller path length of the microfluidic detection chamber (*ca.* 1.8 mM compared to the 10 mM pathlengths of standard cuvettes). According to World Health Organisation the detection limits achievable by spectrometric standard procedures for drinking water are reported to be 0.005–0.010 mg L^{-1} for nitrite [43]. The levels obtained by the portable, integrated microfluidic analytical platform remain lower than the allowable limits, and are therefore useful for quantification as well as threshold testing.

Table 2
Analysis of freshwater samples for nitrite using the portable, integrated microfluidic analytical platform and the UV–vis spectrophotometer ($n=3$).

Water sample no.	**UV–vis spectrophotometer**	**Microfluidic analytical platform**
1	0.010 ± 0.001	0.010 ± 0.003
2	0.410 ± 0.004	0.400 ± 0.006
3	0.420 ± 0.003	0.410 ± 0.009
4	0.380 ± 0.025	0.310 ± 0.045

The usefulness of the proposed portable integrated microfluidic analytical platform for the determination of traces of nitrite in freshwater samples obtained from Tolka River, Ireland, was evaluated using our system and UV–vis spectrophotometer, for comparison. Table 2 shows that there is very good correlation between the bench top instrument and the portable platform.

4. Conclusions

It has been demonstrated through this study that a light actuated polymer gel microvalve can be operated successfully within a microfluidic channel to perform an assay, and the platform has been successfully applied to the analysis of water samples for nitrite. This could have important implications for the practical implementation of microfluidics, as it potentially opens the way towards the generation of low-cost, photo-controlled microflow systems in which the actuation stimuli can be totally separated from the chemistry, which can be contained within a physically separate and sealed fluidic chip. Full integration of the valve structures is possible, and the ability to create these structures *in situ*, post-fabrication of the fluidic unit, could enable entire fluidic system components to be manufactured at very low cost.

However, in their current form, the PSPNIPAAm ionogel based valves require exposure to acidic solution in order to induce swelling. It should be noted that the shrinking mechanism of the gel results in the release of protons into the external solution around the gel. While this does not affect the chemistry presented in this work, it may affect other assays, for example, enzyme or antibody based methods, or the handling of cells and proteins, which typically require neutral pH. In such cases, the valves may have to be restricted to single use, with the acidic solution pushed through the microfluidic system in front of the assay reagents. Strategies to extend the functional pH range of the valve (currently restricted to around pH 3 for reswelling), and to improve the response time (by increasing the rate of water uptake and release, or increasing the surface area to bulk ratio of the valve structure) are currently being actively investigated. Finally, we have chosen nitrite as the target analyte for demonstrating the functionality of the prototype platform. This can easily be extended to include nitrate (through incorporation of a reduction step), and the wide range of other important analytes for which effective colourimetric methods exist.

Acknowledgements

The authors wish to thank to the Marie Curie Initial Training Network funded by the EC FP7 People Programme, Science Foundation of Ireland under Grant 07/CE/I1147. C.F. acknowledges the support of SFI under the same grant code. This work has been supported by the Science Foundation Ireland under Grant no. 10/CE/B1821.

Appendix A. Supplementary material

Supplementary data associated with this article can be found in the online version at http://dx.doi.org/10.1016/j.talanta.2013.07.058.

References

[1] J. Lucey, Environmental protection agency [electronic resource]: water quality in Ireland 2007–2008: key indicators of the aquatic environment (online) (2009).
[2] S. Ramirez-Garcia, D. Diamond, J. Int. Mater. Syst. Struct. 18 (2007) 159–164.
[3] D. Diamond, K.T. Lau, S. Brady, J. Cleary, Talanta 75 (2008) 606–612.
[4] V.J. Sieben, C.F.A. Floquet, I.R.G. Ogilvie, M.C. Mowlem, H. Morgan, Anal. Methods 2 (2010) 484–491.
[5] United Nations, Environment Programme, Earthscan Publications, London, UK, 2002.
[6] P. Brimblecombe, D.H. Stedman, Nature 298 (1982) 460–462.
[7] M.A. Koupparis, K.M. Walczak, H.V. Malmstadt, Analyst 107 (1982) 1309–1315.
[8] J.E. Melanson, C.A. Lucy, J. Chromatogr. A 884 (2000) 311–316.
[9] J. Davis, M.J. Moorcroft, S.J. Wilkins, R.G. Compton, M.F. Cardosi, Analyst 125 (2000) 737–742.
[10] M.J. Moorcroft, J. Davis, R.G. Compton, Talanta 54 (2001) 785–803.
[11] J. Dutt, J. Davis, J. Env. Monit. 4 (2002) 465–471.
[12] P.H. Petsul, G.M. Greenway, S.J. Haswell, Anal. Chim. Acta 428 (2001) 155–161.
[13] A.K. Hanson, OCEANS 2000 MTS/IEEE Conference and Exhibition, 2000.
[14] N. Sombatsompop, N.S. Intawong, N.T. Intawong, Sens. Actuators A 102 (2002) 76–82.
[15] G.J. Schmidt, R.P.W. Scott, Analyst 109 (1984) 997–1002.
[16] M.A. Feres, B.F. Reis, Talanta 68 (2005) 422–428.
[17] D. Betteridge, W.C. Cheng, E.L. Dagless, P. David, T.B. Goad, D.R. Deans, D. A. Newton, T.B. Pierce, Analyst 108 (1983) 1–16.
[18] V.F. Curto, C. Fay, S. Coyle, R. Byrne, C. O'Toole, C. Barry, S. Hughes, N. Moyna, D. Diamond, F. Benito-Lopez, Sens. Actuators B 171–172 (2012) 1327–1334.
[19] C. Fay, K.-T. Lau, S. Beirne, C. Conaire, K. McGuinness, B. Corcoran, N.E. O'Connor, D. Diamond, S. McGovern, G. Coleman, R. Shepherd, G. Alici, G. Spinks, G. Wallace, Sens. Actuators B 150 (2010) 425–435.
[20] D. Diamond, S. Coyle, S. Scarmagnani, J. Hayes, Chem. Rev. 108 (2008) 652–679.
[21] M. Czugala, R. Gorkin III, T. Phelan, J. Gaughran, V.F. Curto, J. Ducrée, D. Diamond, F. Benito-Lopez, Lab. Chip. 12 (2012) 5069–5078.
[22] M. Czugala, B. Ziolkowski, R. Byrne, D. Diamond, F. Benito-Lopez, in: Proceedingsof SPIE 8107, Nano-Opto-Mechanical Systems (NOMS) (2011) 81070C–81070C.
[23] S. Watabe, M. Tatsuoka, T. Shimomae, Y. Shirasaki, J. Mizuno, T. Funatsu, S. Shoji, in: Proceedings of the 13th International Conference on Solid-State Sensors, Actuators and Microsystems, 2005. Digest of Technical Papers. Transducers 05.
[24] Y. Shirasaki, J. Tanaka, H. Makazu, K. Tashiro, S. Shoji, S. Tsukita, T. Funatsu, Anal. Chem. 78 (2005) 695–701.
[25] H. Nagai, J. Takahashi, S. Wakida, in: Proceedings of the 7th International Conference on Miniaturized Systems for Chemistry and Life Sciences (uTAS2003), 2003.
[26] G.L. Liu, J. Kim, Y. Lu, L.P. Lee, Nat. Mater. 5 (2006) 27–32.
[27] S.R. Sershen, G.A. Mensing, M. Ng, N.J. Halas, D.J. Beebe, J.L. West, Adv. Mat. 17 (2005) 1366–1368.
[28] S. Sugiura, K. Sumaru, K. Ohi, K. Hiroki, T. Takagi, T. Kanamori, Sens. Actuators A 140 (2007) 176–184.
[29] T. Satoh, K. Sumaru, T. Takagi, T. Kanamori, Soft Matter 7 (2011) 8030–8034.
[30] I.M.P. de Vargas-Sansalvador, C. Fay, T. Phelan, M.D. Fernandez-Ramos, L.F. Capitan-Vallvey, D. Diamond, F. Benito-Lopez, Anal. Chim. Acta 699 (2011) 216–222.
[31] C. Fay, A.R. Doherty, S. Beirne, F. Collins, C. Foley, J. Healy, B.M. Kiernan, H. Lee, D. Maher, D. Orpen, T. Phelan, Z. Qiu, K. Zhang, C. Gurrin, B. Corcoran, N.E. O'Connor, A.F. Smeaton, D. Diamond, Sensors 11 (2011) 6603–6628.
[32] M. O' Toole, R. Shepherd, K.T. Lau, D. Diamond, Proc. SPIE 6755 (2007) 67550P.
[33] M.F. Mims, Sci. Am. 263 (1990) 106–109.
[34] K.T. Lau, S. Baldwin, R.L. Shepherd, P.H. Dietz, W.S. Yerzunis, D. Diamond, Talanta 63 (2004) 167–173.
[35] J. MacFaddin, Nitrate/Nitrite Reduction Tests, in: Biochemical Tests for Identification of Medical Bacteria, 3rd ed., Lippincott Williams & Wilkins, Philadelphia, 2000.
[36] K. Sumaru, M. Kameda, T. Kanamori, T. Shinbo, Macromolecules 37 (2004) 4949–4955.
[37] M. O'Toole, D. Diamond, Sensors 8 (2008) 2453–2479.
[38] P.K. Dasgupta, I.-Y. Eom, K.J. Morris, J. Li, Anal.Chim.Acta 500 (2003) 337–364.
[39] M. O' Toole, K.T. Lau, R. Shepherd, C. Slater, D. Diamond, Anal Chim. Acta 567 (2007) 290–294.
[40] O. Brand, Proc IEEE 94 (2006) 1160–1176.
[41] D. Tse, P. Viswanath, Cambridge University Press, 2005.
[42] D. Diamond, V.C.A. Hanratty, Spreadsheet Applications for Chemistry Using Microsoft Exel, John Wiley and Sona, New York, 1997.
[43] World Health Organization, Guidelines for drinking-water quality [electronic resource]: incorporating 1st and 2nd addenda, vol. 1, Recommendations, Geneva, 2008.